Nutrition and Cancer

ISSN: (Print) (Online) Journal homepage: https://www.tandfonline.com/loi/hnuc20

The Natural Alkaloid Piperlongumine Inhibits Metastatic Activity and Epithelial-to-Mesenchymal Transition of Triple-Negative Mammary Carcinoma Cells

Leanne M. Delaney , Nathan Farias , Javad Ghassemi Rad , Wasundara Fernando , Henry Annan & David W. Hoskin

To cite this article: Leanne M. Delaney , Nathan Farias , Javad Ghassemi Rad , Wasundara Fernando , Henry Annan & David W. Hoskin (2020): The Natural Alkaloid Piperlongumine Inhibits Metastatic Activity and Epithelial-to-Mesenchymal Transition of Triple-Negative Mammary Carcinoma Cells, Nutrition and Cancer, DOI: 10.1080/01635581.2020.1825755

To link to this article: https://doi.org/10.1080/01635581.2020.1825755

Published online: 05 Oct 2020.

NUTRITION AND CANCER
https://doi.org/10.1080/01635581.2020.1825755

Taylor & Francis
Taylor & Francis Group

The Natural Alkaloid Piperlongumine Inhibits Metastatic Activity and Epithelial-to-Mesenchymal Transition of Triple-Negative Mammary Carcinoma Cells

Leanne M. Delaney[a], Nathan Farias[a], Javad Ghassemi Rad[b], Wasundara Fernando[b], Henry Annan[a], and David W. Hoskin[a,b,c]

[a]Department of Microbiology and Immunology, Faculty of Medicine, Dalhousie University, Halifax, Nova Scotia, Canada; [b]Department of Pathology, Faculty of Medicine, Dalhousie University, Halifax, Nova Scotia, Canada; [c]Department of Surgery, Faculty of Medicine, Dalhousie University, Halifax, Nova Scotia, Canada

ABSTRACT

In this study, we determined the effect of low dose piperlongumine on the motility/invasive capacity and epithelial-to-mesenchymal transition (EMT) of MDA-MB-231 triple-negative breast cancer (TNBC) cells and the metastasis of 4T1 mouse mammary carcinoma cells. MTT assays measured the effect of piperlongumine on TNBC cell growth. Motility/invasiveness were determined by gap closure/transwell assays. Western blotting assessed ZEB1, Slug, and matrix metalloproteinase (MMP) 9 expression. Interleukin (IL) 6 was detected by ELISA. MMP2, E-cadherin, and miR-200c expression was determined by real-time quantitative polymerase chain reaction. Reactive oxygen species (ROS) were measured by flow cytometry. The orthotopic 4T1 mouse model of breast cancer was used to examine metastasis. Piperlongumine-treated MDA-MB-231 cells showed reduced motility/invasiveness, decreased MMP2 and MMP9 expression, increased miR-200c expression, reduced IL-6 synthesis, decreased expression of ZEB1 and Slug, increased E-cadherin expression, and epithelial-like morphology. Piperlongumine also inhibited transforming growth factor β-induced ZEB1 and Slug expression. ROS accumulated in piperlongumine-treated cells, while changes in metastasis-associated gene expression were ablated by exogenous glutathione. Metastasis of 4T1 cells to the lungs of BALB/c mice was dramatically reduced in piperlongumine-treated animals. These findings reveal a previously unknown capacity of low dose piperlongumine to interfere with TNBC metastasis via an oxidative stress-dependent mechanism.

ARTICLE HISTORY
Received 13 July 2020
Accepted 11 September 2020

Introduction

Triple-negative breast cancer (TNBC), which lacks receptors for estrogen and progesterone and does not overexpress human epidermal growth factor receptor 2 (HER2), has a poor prognosis upon recurrence and is a leading cause of breast cancer-related death in women (1). The progression to metastatic disease together with the development of resistance to chemotherapy and the lack of targeted therapies are major contributors to poor patient outcomes. As a result, new cancer therapeutics are being sought that target the cellular changes associated with metastasis and drug resistance. Potential targets include growth factor signaling pathways, cell-to-cell communication, stromal-cell interactions, and cytokine signals involved in epithelial-to-mesenchymal transition (EMT) by breast cancer stem cells that results in new tumor growth at secondary sites (2,3). EMT involves the loss of epithelial properties such as cellular adhesion junctions and the acquisition of mesenchymal properties, resulting in motile and invasive cells that are able to escape the primary tumor, travel to distant tissues, and reconstitute new tumors with even greater genetic and phenotypic heterogeneity than the primary tumor (4). The transforming growth factor (TGF) β pathway is critical for the induction of EMT since receptor engagement leads to the nuclear translocation of Smad protein and the subsequent upregulation of EMT-inducing transcription factors Twist, Slug, Snail, and zinc finger E-box binding protein (ZEB) 1 and 2 proteins (5,6). Breast cancer cell EMT activation, invasion and metastasis are also promoted by the aberrant expression of matrix metalloproteinases (MMP) (7).

CONTACT David W. Hoskin d.w.hoskin@dal.ca Department of Pathology, Dalhousie University, 5850 College St., PO Box 15000, Halifax, Nova Scotia, B3H 4R2, Canada

The pungent fruits of the long pepper plant (*Piper longum*) are widely consumed as a spice, as well as being used in traditional medicine to treat a variety of ailments (8). Long pepper plant fruits contain piperlongumine, a bioactive alkaloid that selectively kills breast cancer cells and other cancer cell types (9–12). The cytotoxic activity of piperlongumine has been attributed to oxidative stress caused by increased levels of hydrogen peroxide in piperlongumine-treated cancer cells (13). Cancer cells typically have a greater reactive oxygen species (ROS) burden and are therefore more sensitive than normal cells to oxidative stress (14). Piperlongumine also inhibits the JAK2-STAT3 (15), nuclear factor (NF) κB (16), and phosphatidylinositol 3-kinase/Akt/mammalian target of rapamycin signaling pathways (17), reduces overall nuclear traffic (18), and activates pro-apoptotic C/EBP homologous protein (9), mitogen-activated protein kinase p38 and phospho-c-Jun N-terminal kinase (11). However, the effect of noncytotoxic low dose piperlongumine on metastasis-associated molecules and activities of TNBC cells has not been fully investigated.

In this study, we investigated the impact of subcytotoxic low dose piperlongumine on the motility and invasiveness of triple-negative MDA-MB-231 breast cancer cells. We also determined the effect of piperlongumine treatment on the expression of EMT-associated proteins by MDA-MB-231 cells and whether piperlongumine-induced ROS accumulation was involved. The 4T1 orthotopic mouse mammary carcinoma model of metastasis was used to assess the impact of piperlongumine treatment on the metastasis of 4T1 cells from the mammary fat pad to the lungs.

Materials and Methods

Reagents

Piperlongumine was purchased from EMD Millipore Corp. (Billerica, MA, USA) and was stored at stock concentrations of 20 mM in dimethyl sulfoxide (DMSO) at −20 °C. Bovine serum albumin, collagenase, fibronectin, DMSO, DNAse I, regular and phenol red-free Dulbecco's Modified Eagle's Medium (DMEM), Hanks' Balanced Salt Solution (HBSS), phosphate buffered saline (PBS), elastase, reduced glutathione (GSH), leupeptin, mitomycin C, 3-(4,5-dimethylthiazol-2-yl)-2,5-diphenyltetrazolium bromide (MTT), Nonidet P-40, pepstatin A, phenylarsine oxide, phenylmethylsulfonyl fluoride, sodium deoxycholate, sodium fluoride, 6-thioguanine, and Triton X-100 were all from Sigma-Aldrich Canada (Oakville, ON). Invitrogen Canada Inc. (Burlington, ON) supplied 5-(and-6)-chloromethyl-2′,7′-dichlorodihydrofluorescein diacetate, acetyl ester (DCFDA). Acrylamide/bisacrylamide (29:1, 30% solution), ammonium persulfate, ethylene glycol tetraacetic acid, paraformaldehyde, sodium dodecyl sulfate (SDS), tetramethylethylenediamine, Tris base, and Tween-20 were from Bio-Shop Canada Inc. (Burlington, ON). Anti-human ZEB1, Slug and E-cadherin rabbit monoclonal antibodies (mAb), and anti-human β-actin antibody (Ab) were from Cell Signaling Technology Inc. (Beverly, MA). Rabbit anti-human MMP9 mAb and horse radish peroxidase (HRP)-conjugated donkey anti-rabbit IgG Ab were from Santa Cruz Biotechnology (Santa Cruz, CA). Human TGFβ1 was from Peprotech (Dollard des Ormeaux, QC).

Cell Lines and Culture

MDA-MB-231 human mammary adenocarcinoma cells were provided by Dr. S. Drover (Memorial University of Newfoundland, St. John's, NL). BT-549 and Hs578T human mammary carcinoma cells were from ATCC (Manassas, VA, USA). 4T1 murine mammary carcinoma cells were from Dr. D. Waisman (Dalhousie University, Halifax, NS). Mammary carcinoma cell lines were authenticated by short tandem repeat analysis conducted by ATCC and DDC Medical/Division of DNA Diagnostics Center (Fairfield, OH). Mammary carcinoma cells were cultured in DMEM supplemented with 10% heat-inactivated fetal bovine serum (FBS), 5 mM HEPES at pH 7.4, 2 mM L-glutamine, 100 U/ml penicillin, and 100 µg/ml streptomycin (all from Invitrogen Canada Inc., Burlington, ON), maintained at 37 °C in a 10% CO_2 humidified atmosphere and passaged every 4 days.

MTT Assay

Metabolic activity was measured by colorimetric MTT assays as an indicator of cell viability. MDA-MB-231, BT-549, Hs578T or 4T1 cells were seeded into quadruplicate wells of a 96-well flat-bottom plate at 5×10^3 cells/well and allowed to adhere overnight. Cells were then treated with medium alone, vehicle (DMSO) or increasing concentrations of piperlongumine. After culture for 48 h, MTT (final concentration 0.5 µg/ml) was added to each culture and cells were incubated for another 2 h. Cell-free supernatants were then discarded and 0.1 ml DMSO was added to each well to solubilize formazan crystals. Absorbance at 570 nm was measured using an ELX800 UV Universal Microplate Reader

(BIO-TEK Instruments Inc., Winooski, VT). Values were normalized to the medium control.

Gap Closure Assay

The motility of MDA-MB-231 cells in the absence or presence of piperlongumine was measured using a gap closure assay. MDA-MB-231 cells at 1×10^6 cells/ml were seeded into each chamber of a 2-chamber silicone insert (Ibidi, Munich, Germany) containing a cell-free gap measuring 500 µm, allowed to proliferate for 12 h and then treated with 10 µg/ml mitomycin C in complete DMEM for 2 h to arrest cell cycle. Mitomycin C was removed and replaced with complete DMEM. Cells were cultured for 12 h, after which medium alone, vehicle (DMSO) or 2.5 µM piperlongumine was added and cells were cultured for another 16 h to allow gap closure. Images were taken using a Nikon® Digital Sight camera connected to a Nikon® Eclipse T5100 microscope (Nikon Canada, Mississauga, ON). Gap closure efficiency was measured by quantifying pixel density within the 500 µm gap using Image J software (NIH).

Transwell Invasion Assay

MDA-MB-231 cells were seeded into 75 mm^2 flasks at 1×10^6 cells/flask and allowed to adhere for 12 h. Medium alone, vehicle (DMSO) or 1 µM piperlongumine was then added to flasks and cells were cultured for 36 h, after which cultures were serum-starved for 12 h. MDA-MB-231 cells were harvested, resuspended in serum-free DMEM at 1×10^6 cells/ml, and added to the upper chamber of a 48-well transwell plate (Neuro Prob, Gaithersburg, MD). The upper chamber was separated from the lower chamber by an 8 µm porous polycarbonate membrane coated with fibronectin (0.5% w/v). Wells containing serum-free DMEM in the lower chamber were used as the negative control. Test wells contained DMEM plus FBS as a chemoattractant in the lower chamber. Cells were cultured for 12 h at 37 °C in a 10% CO_2 humidified atmosphere to allow cells to migrate across the fibronectin-coated membrane. Migrated cells on the bottom of the membrane were stained using a Diff-Quik staining kit (VWR, Radnor, PA). Membranes were mounted onto slides and migration was quantified using Image J software to measure pixel density in pictures of five random fields of view captured using a Nikon® Digital Sight camera connected to a Nikon® Eclipse T5100 microscope.

Real-Time Quantitative Polymerase Chain Reaction (RT-qPCR)

MDA-MB-231 cells were seeded into 75 mm^2 flasks at 1×10^6 cells/flask and allowed to adhere for 12 h. Medium alone, vehicle (DMSO) or piperlongumine (1 or 2.5 µM) was then added to flasks and cells were cultured for 48 or 72 h. RNA was extracted from cells using a Qiagen RNeasy® Mini Kit, according to the manufacturer's instructions (Qiagen, Toronto, ON). RNA purity was confirmed using a Thermo Fisher Scientific Nanodrop 2000 spectrophotometer (Dartmouth, NS). RNA was stored at −80 °C. The cDNA was generated from 667 ng RNA using the BioRad iScript cDNA Synthesis Kit, according to the manufacturer's instructions (Bio-Rad, Hercules, CA). Real-time PCR was performed using the Qiagen Quantifast SYBR® Green method and a Corbett Research Rotor-Gene 6000 series analyzer (Corbett Life Science, Concorde, Australia). Cycling conditions were as follows: 5 min initial heat activation at 95 °C, 10 sec denaturation at 95 °C and 30 sec extension at 60 °C. Primer sequences were as follows:

MMP2 – Forward: 5′-TGG CAA GTA CGG CTT CTG TC-3′; Reverse: 5′-TTC TTG TCG CGG TCG TAG TC-3′

E-cadherin – Forward:5′- CAG CCA CAG ACG CGG ACG AT-3′; Reverse: 5′-CTC TCG GTC CAG CCC AGT GGT −3′

Glyceraldehyde-3-phosphate dehydrogenase (GAPDH) - Forward: 5′-GAG TCA ACG GAT TTG GTC GT-3′; Reverse: 5′-TTG ATT TTG GAG GGA TCT CG-3′

Forty cycles were used, and a melt curve analysis was performed. All PCR reactions were performed in triplicate. Data was analyzed using the Rotor-Gene 6000 series software program.

miRNA Analysis

The Qiagen miScript miRNA PCR System was used to measure miR-200c expression by MDA-MB-231 cells cultured, as described above, for 72 h in the absence or presence of 2.5 μM piperlongumine. Total RNA, containing miRNA, was extracted from vehicle- or piperlongumine-treated MDA-MB-231 cells using the Qiagen miRNeasy® Mini Kit. The cDNA was prepared using the Qiagen miScript II RT Kit, and miR-200c expression was measured with the Qiagen miScript Primer Assay.

Western Blot Analysis

MDA-MB-231 cells were seeded into 75 mm^2 flasks at 1×10^6 cells/flask and allowed to adhere for 12 h. Medium alone, vehicle (DMSO) or piperlongumine (0.5, 1, or 2.5 μM) was then added to flasks and cells were cultured for 48 h. Following treatment, cells were harvested, washed with PBS, and resuspended in ice-cold lysis buffer (1% Nonidet P-40 (v/v), 0.5% sodium deoxycholate (w/v), 0.1% SDS (w/v), 20 mM Tris, 150 mM NaCl, 1 mM ethylene diamine tetraacetic acid, 1 mM ethylene glycol tetraacetic acid at pH 7.5) containing a protease inhibitor cocktail (5 μg/ml leupeptin, 5 μg/ml pepstatin A, 10 μg/ml aprotinin, 100 μM sodium orthovanadate, 1 mM dithiothreitol, 10 mM sodium fluoride, 10 μM phenylarsine oxide, and 1 mM phenylmethylsulfonyl fluoride, all from Sigma-Aldrich Canada) for 15 min at 4 °C. Cell lysates were cleared by centrifugation at 14,000 *g* for 10 min at 4 °C, supernatant was collected and total protein was quantified using a Bradford Assay Kit (Bio-Rad). Cell lysates were then diluted 1:1 in denaturing buffer (187.5 M Tris–HCl, 30% glycerol (v/v), 6% SDS (w/v), 15% β-mercaptoethanol (v/v), 0.015% bromophenol blue (w/v)) and kept at 95 °C for 5 min. Then 40 μg of protein was loaded into wells of a 10% SDS-polyacrylamide gel and electrophoresed at 120 V for 1.5 h. Proteins were transferred to PVDF membranes using the iBlot® gel transfer device (Invitrogen) and membranes were then blocked for 1 h at room temperature in 5% skim milk (w/v) in Tween-20 Tris-buffered saline (200 mM Tris, 1.5 M NaCl, pH 7.6, 0.1% Tween-20 (v/v)). Blots were probed overnight at 4 °C with primary mAb (1:1000 dilution) in blocking buffer. Membranes were washed thoroughly with Tween-20 Tris-buffered saline at room temperature and then probed for 1 h at room temperature with HRP-conjugated donkey anti-rabbit IgG Ab (1:10,000 dilution) in blocking buffer. Equal protein loading was confirmed by probing for β-actin expression. Protein bands were visualized with chemiluminescent HRP substrate Luminata™ (Millipore, Darmstadt, Germany) and Amersham high performance chemiluminescence film (GE Healthcare, Buckinghamshire, UK). Image Studio Software was used for densitometric analysis.

Measurement of Intracellular ROS

MDA-MB-231 cells were seeded into 6-well plates at 1×10^5 cells/well and cultured overnight to support cell adhesion. Cells were then stained for 30 min at 37 °C with 10 μM DCFDA prepared in serum-free and phenol red-free DMEM. Cells were rinsed with warm PBS to remove excess stain and treated with 1% FBS-supplemented and phenol red-free DMEM alone, vehicle (DMSO) or piperlongumine (0.5, 1.0 and 2.5 μM) for 4 or 6 h. Cells were harvested, washed, and resuspended in PBS. Fluorescence intensity of 1×10^4 events was measured using a FACSCanto flow cytometer (Becton Dickinson, San Jose, CA).

Interleukin (IL)-6 Enzyme-Linked Immunosorbent Assay (ELISA)

MDA-MB-231 cells were seeded into a 24-well plate at 2.5×10^5 cells/well and allowed to adhere for 12 h. Medium alone, vehicle (DMSO) or 2.5 μM piperlongumine) was then added to wells and cells were cultured for 48 h. Cell-free supernatants were harvested and IL-6 was measured by ELISA, according to the manufacturer's instructions (eBioscience, San Diego, CA). Absorbance at 450 nm was determined using an ELX800 UV Universal Microplate Reader and data were plotted on a standard curve using SOFTmax® PRO Software (Molecular Devices Corp., Sunnyvale, CA).

Immunofluorescence

MDA-MB-231 cells were seeded onto sterile glass slides, allowed to adhere and cultured for 72 h in the presence of the vehicle (DMSO) or 2.5 μM piperlongumine. Cell monolayers were washed with PBS and fixed in 4% paraformaldehyde (w/v) for 15 min at room temperature. Cell monolayers were then thoroughly washed with PBS, blocked with 3% (w/v) bovine serum albumin, and permeabilized for 20 min in Tris-buffered saline containing 3% (w/v) bovine serum albumin and 0.3% Triton-X-100 (v/v). Cell monolayers on slides were incubated in the dark with 200 nM phalloidin-Alexafluor 488 (Thermo Fisher Scientific) for 15 min to visualize F-actin. Cells were then incubated with 100 nM DAPI stain for 5 min in the dark to visualize nuclei. After thorough washing with PBS and one wash with water, fluorescence mounting medium (Dako North America Inc., Carpinteria, CA) was added to the cell monolayers followed by coverslips. Images were captured at 40× magnification with a Zeiss Axio Imager Z2 (Carl Zeiss Canada Ltd., Toronto, ON).

4T1 Mouse Model of Metastatic Breast Cancer

Orthotopic transplantation of triple-negative 4T1 mouse mammary carcinoma cells into a mammary fat pad of syngeneic female BALB/c mice results in extensive metastasis of tumor cells from the primary tumor

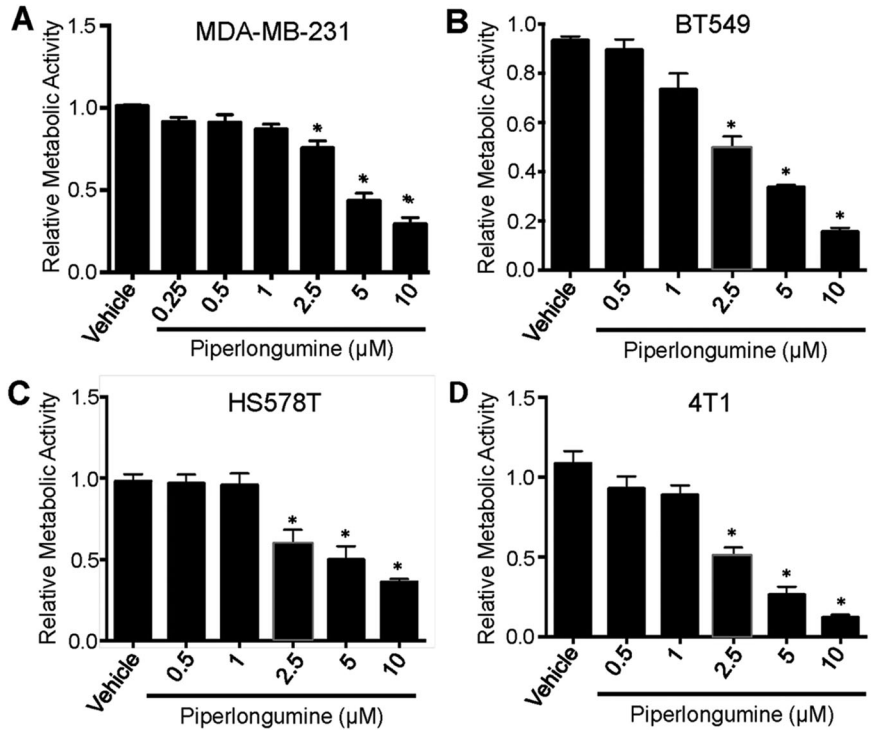

Figure 1. Dose-dependent inhibition of triple-negative mammary carcinoma cell growth by piperlongumine. (A) MDA-MB-231, (B) BT549, (C) Hs578T and (D) 4T1 mammary carcinoma cells were cultured in the presence of medium, vehicle (DMSO) or the indicated concentrations of piperlongumine for 48 h. Cell growth/viability was then measured using an MTT assay. Data shown are the average of 3 independent experiments ± the standard error of the mean (SEM). Statistical significance relative to the vehicle control was determined by ANOVA with Dunnett's post-hoc test; * denotes $p < 0.01$.

to the lungs (19). Six-to-eight-week-old female BALB/c mice were purchased from Charles River Canada (Lasalle, QC, Canada) and housed in the Carleton Animal Care Facility. Ethics approval was obtained from the Dalhousie University Committee on Laboratory Animals, in accordance with Canadian Council of Animal Care guidelines. Mice were injected with 1×10^5 4T1 cells in the left inguinal mammary fat pad and randomly assigned to control and treatment groups (11 mice/group). Tumor size was measured every day using digital calipers to determine the longest diameter (L) and diameter perpendicular to longest diameter (P); volume was calculated using (L x P^2)/2. Once the tumors reached a volume of 100 mm^3, typically at 8 day post implantation, mice received 0.05% (v/v) DMSO in PBS (control group) or 2.5 mg/kg piperlongumine in PBS (treatment group) for 9 days via daily intraperitoneal injection. The dose of piperlongumine was calculated to be sub-cytotoxic, assuming systemic distribution. Mice were then euthanized, and tumors were excised, weighed, photographed, and fixed in 10% (v/v) acetate-buffered formalin. Lungs were harvested and mechanically homogenized in HBSS. Digestion buffer (0.75 mg/ml collagenase, 0.05 mg/ml elastase, 0.05 mg/m DNAse I in HBSS) was then added and the tissue preparation was incubated at 37 °C for 1 h, after which the digested tissue was washed and passed through a cell strainer prior to centrifugation for 5 min at 500 *g*. Cells were resuspended in complete DMEM containing 60 μM 6-thioguanine to select for 6-thioguanine-resistant 4T1 cells, and seeded into 10 cm cell culture dishes in multiple dilutions. Cells were cultured for 2 weeks at 37 °C in a 10% CO_2 humidified atmosphere. At the end of culture, the adherent 4T1 cells were washed with PBS and stained with 0.4% (w/v) crystal violet to visualize colonies.

Histology and Immunohistochemistry

Fixed tumors were embedded in paraffin and sectioned into 5 μm-thick slices that were mounted onto glass slides. Some tumor sections were stained with hematoxylin and eosin to visualize live and necrotic cells. Other tumor sections were deparaffinized with xylene and rehydrated with graded ethanol to water addition. Heat-mediated antigen retrieval with sodium acetate (pH 6.0) was performed, followed by incubation in hydrogen peroxide solution. Tumor sections were blocked with Rodent M Block (Biocare Medical, Pacheco, CA) and incubated with anti-MMP2 mAb or anti-Ki67 mAb (both from Abcam, Toronto, ON) overnight at room temperature. MMP2-stained tumor

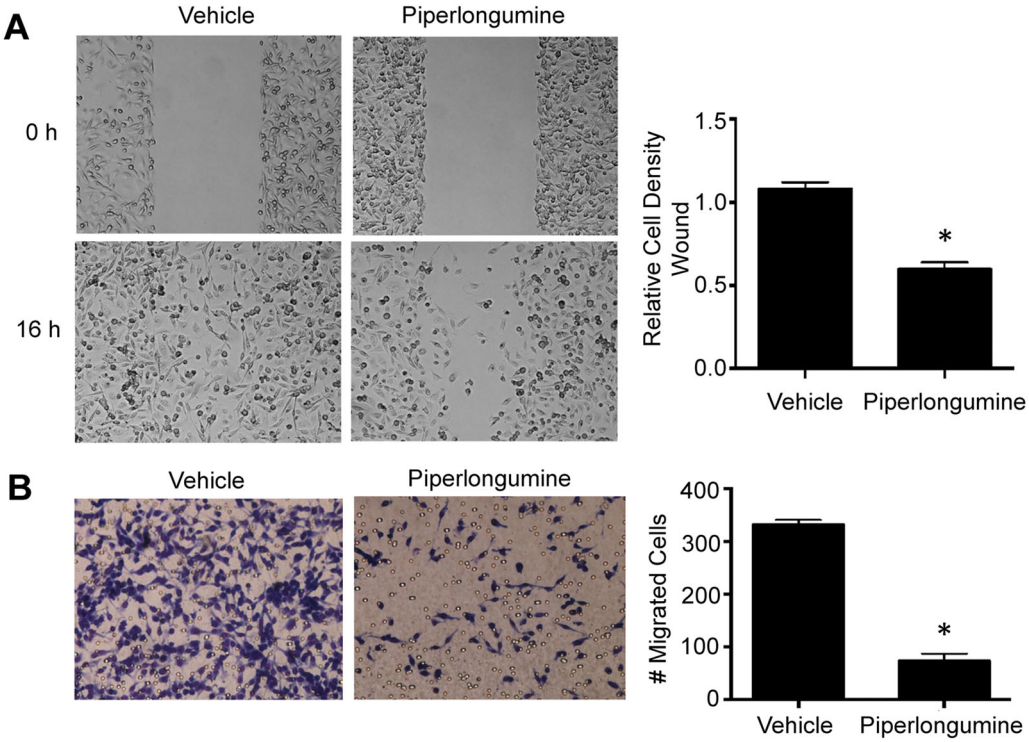

Figure 2. Piperlongumine inhibits TNBC cell motility and invasion. (A) MDA-MB-231 cells were plated in cell culture inserts and cell cycle was arrested by mitomycin C treatment (10 μg/ml). After 24 h culture in the presence of medium, vehicle (DMSO), or piperlongumine (2.5 μM), cell culture inserts were removed, and cells were allowed to close the resulting gap for 16 h. Image J software was used to measure the final gap width. (B) MDA-MB-231 cells were grown in the presence of medium, vehicle (DMSO), or piperlongumine (1 μM) for 24 h prior to serum-starvation and transfer to the upper wells of a 48-well Boyden chamber at 5×10^4 cells/well. A fibronectin-coated 8 μm porous polycarbonate membrane separated the upper wells from the lower wells containing DMEM with or without FBS as a chemoattractant. Cells that migrated through this membrane after 16 h of culture were stained with crystal violet and counted. (A, B) Data shown are the average of 3 independent experiments ± SEM. Statistical significance relative to the vehicle control was determined by Student's t-test; * denotes $p < 0.001$.

sections were incubated with mouse-on-mouse HRP-Polymer (Biocare Medical) and detected using the HRP/DAB detection system (Dako, Carpinteria, CA). Ki67-stained tumor sections were incubated with MACH 4 MR AP Polymer and detected using the Vulcan Fast Red Chromogen Kit 2 (both from Biocare Medical).

Statistical Analysis

GraphPad Prism software (GraphPad Software Inc., La Jolla, CA, USA) was used to perform Student's t-test or ANOVA with Dunnett's or Tukey's post-hoc tests, as appropriate; $p < 0.05$ was considered statistically significant.

Results

Piperlongumine Reduces Metastatic Characteristics of TNBC Cells

MDA-MB-231, BT-549, and Hs578T TNBC cells, as well as 4T1 mouse triple-negative mammary carcinoma cells were exposed to increasing concentrations of piperlongumine to determine a sub-cytotoxic dose. As shown in Figure 1, dose-dependent growth inhibition was observed in MDA-MB-231, Hs578T, BT459, and 4T1 cell cultures treated with piperlongumine. Exposure to 10 μM piperlongumine caused at least a 50% decrease in the metabolic activity of all cell lines tested. MDA-MB-231 cells were relatively resistant to piperlongumine, exhibiting little or no growth inhibition in the presence of 1 or 2.5 μM piperlongumine. All subsequent in vitro experiments therefore used highly metastatic MDA-MB-231 cells that were cultured in the absence or presence of a sub-cytotoxic concentration (1 or 2.5 μM) of piperlongumine.

To investigate the effect of piperlongumine on the metastatic potential of TNBC cells, we compared the motility and invasiveness of MDA-MB-231 cells that were cultured in the absence or presence of sub-cytotoxic piperlongumine. Figure 2A shows that piperlongumine-treated MDA-MB-231 cells experienced a significant reduction in motility over 16 h in a gap

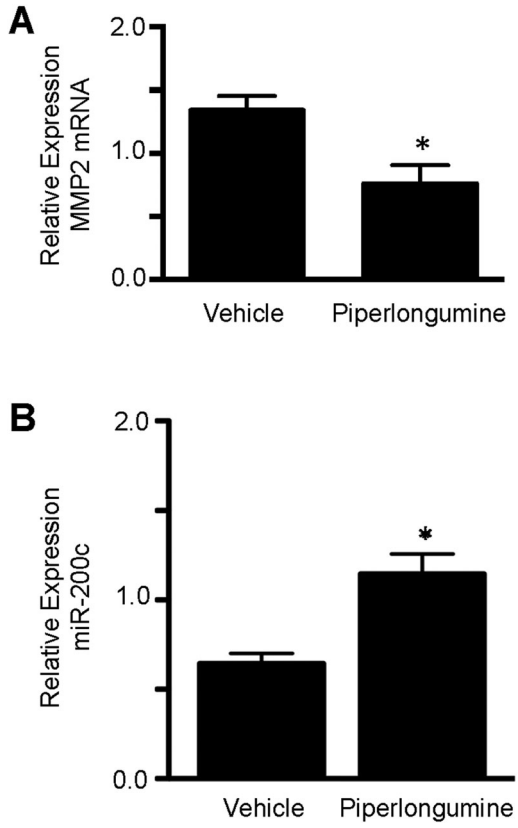

Figure 3. Piperlongumine inhibits MMP2 mRNA expression and promotes miR-200c expression by TNBC cells. (A) MDA-MB-231 cells were cultured for 48 h in the presence of medium, vehicle (DMSO), or 1 μM piperlongumine. (B) MDA-MB-231 cells were cultured for 72 h in the presence of medium, vehicle (DMSO), or 2.5 μM piperlongumine. (A, B) MMP2 mRNA and miR-200c levels were measured using RT-qPCR. Data shown are the average of 3 independent experiments ± SEM. Statistical significance relative to the vehicle control was determined by Students t-test; * denotes $p < 0.05$.

closure assay. Figure 2B shows that stimulus-induced directed migration of MDA-MB-231 cells across a fibronectin-coated membrane was dramatically reduced in the presence of piperlongumine. Expression of MMP2 mRNA (Figure 3A) and MMP9 protein (Figure 7B) was inhibited when MDA-MB-231 cells were treated with the same low dose of piperlongumine. In contrast, Figure 3B shows increased expression of miR-200c in piperlongumine-treated MDA-MB-231 cells. Treatment with low dose piperlongumine also caused a significant decrease in MDA-MB-231 synthesis of IL-6 (Figure 7C). Collectively, these findings suggest that piperlongumine reduces the metastatic potential of breast cancer cells at concentrations that do not substantially impair cell growth.

Piperlongumine Suppresses EMT

We next determined whether molecular markers of EMT were altered following the exposure of TNBC cells to low dose piperlongumine. Western blot analysis revealed that expression of the EMT-promoting ZEB1 and Slug transcription factors was significantly downregulated in piperlongumine-treated MDA-MB-231 cells (Figure 4A and Figure 4B, respectively). In contrast, RT-qPCR analysis showed that E-cadherin mRNA expression was increased in piperlongumine-treated MDA-MB-231 cells (Figure 4C). Next, F-actin and the nucleus of MDA-MB-231 cells were stained with phalloidin-Alexa Fluor 488 and DAPI, respectively, to visualize cell morphology. As shown in Figure 4D, MDA-MB-231 cells normally exhibit mesenchymal-like morphology; however, 72-h culture in the presence of sub-cytotoxic piperlongumine caused the cells to acquire an epithelial-like morphology, which was consistent with the observed alterations in ZEB1, Slug, and E-cadherin expression.

Piperlongumine Prevents TGFβ-Induced Upregulation of ZEB1 and Slug Expression

We used western blot analysis to determine the impact of low dose piperlongumine treatment on TGFβ-induced upregulation of ZEB1 and Slug expression by MDA-MB-231 cells. Figure 5 shows that ZEB1 (Figure 5A) and Slug (Figure 5B) expression was increased when MDA-MB-231 cells were cultured for 48 h in the presence of 1 ng/ml TGFβ, an effect that was abrogated when low dose piperlongumine was added to culture at the same time as TGFβ. Piperlongumine therefore interfered with the ability of TGFβ to induce expression of EMT-promoting transcription factors.

ROS Mediate the Effects of Piperlongumine on EMT- and Metastasis-Related Protein Expression

Flow cytometric analysis of DCFDA-stained MDA-MB-231 cells following treatment with sub-cytotoxic piperlongumine revealed a significant increase in intracellular ROS after only 4 h (Figure 6). To determine whether piperlongumine-induced ROS were the cause of altered EMT- and metastasis-related protein expression, we treated MDA-MB-231 cell cultures with the antioxidant GSH prior to the addition of piperlongumine. As shown in Figure 7, GSH reversed the inhibitory effect of piperlongumine on MMP2 mRNA (Figure 7A) and MMP9 protein (Figure 7B) expression, as well as IL-6 synthesis by piperlongumine-treated MDA-MB-231 cells (Figure 7C). In addition, GSH restored the expression of ZEB1 and Slug protein (Figure 8A), as well as E-cadherin mRNA (Figure 8B), to control levels in MDA-MB-231 cells that were exposed to piperlongumine. These findings

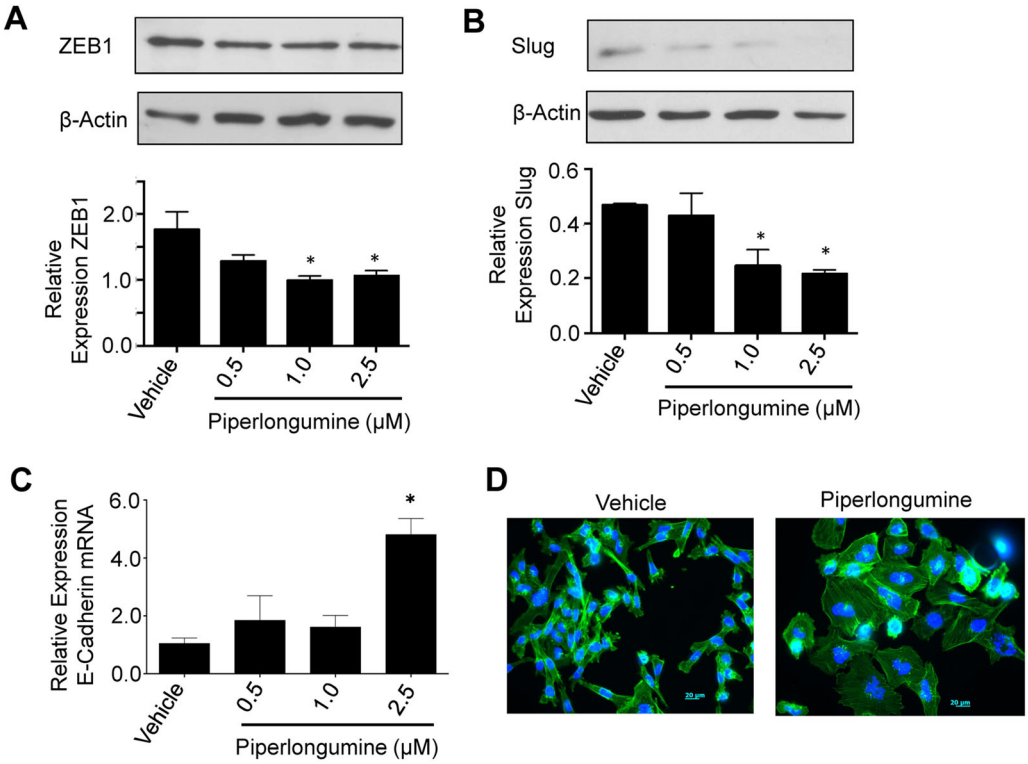

Figure 4. Piperlongumine inhibits EMT and promotes epithelial morphology of TNBC cells. MDA-MB-231 cells were cultured for 48 h in the presence of medium, vehicle (DMSO), or the indicated concentrations of piperlongumine. Cell lysates were prepared and (A) ZEB1 or (B) Slug protein expression was measured by western blotting and densitometry. β-actin expression was determined to confirm equal loading of proteins. Representative blots are shown. (C) MDA-MB-231 cells were cultured for 72 h in the presence of medium, vehicle (DMSO) or the indicated concentrations of piperlongumine. mRNA was isolated and RT-qPCR was used to measure E-cadherin mRNA expression. (A, B, C) Data shown are the average of 3 independent experiments ± SEM. Statistical significance relative to the vehicle control was determined by ANOVA with Dunnett's post-hoc test; * denotes $p < 0.05$. (D) MDA-MB-231 cells were cultured in the presence of vehicle (DMSO) or 2.5 μM piperlongumine for 72 h. F-actin (green) and the nucleus (blue) were then stained with phalloidin-Alexa Fluor 488 and DAPI, respectively, and photographed. A representative image is depicted.

suggest that low-dose piperlongumine suppressed the metastatic activities of MDA-MB-231 cells via ROS generation.

Piperlongumine Inhibits Mouse Mammary Carcinoma Cell Metastasis

Finally, we determined whether the in vitro inhibitory effects of low dose piperlongumine on TNBC motility, invasion and EMT translated to reduced metastasis in vivo. We administered vehicle (DMSO) or piperlongumine (2.5 mg/kg) via daily intraperitoneal injection for 9 days to 4T1 tumor-bearing female BALB/c mice. At the end of treatment, there was no significant difference in primary tumor weight between vehicle- and piperlongumine-treated animals (Figure 9A), indicating that the concentration of piperlongumine used was not cytotoxic to 4T1 cells in vivo. In contrast, there was a significant reduction in lung metastases in piperlongumine-treated mice (Figure 9B), which was independent of the weight of the primary tumor (Figure 9C). Primary tumors from vehicle- and piperlongumine-treated animals had similar areas of live cells and necrotic cells, as well as expression of the Ki67 proliferation marker; however, consistent with our in vitro results, MMP2 expression was reduced in primary tumors from the piperlongumine-treated group. Taken together, these findings suggest that a sub-cytotoxic dose of piperlongumine prevented metastasis in a mouse model of TNBC.

Discussion

Piperlongumine shows promise as a selective anticancer compound due to its capacity to induce apoptosis in cancer cells while sparing normal cells (11,12). Our finding that piperlongumine inhibited the growth of four different triple-negative mammary carcinoma cell lines is in line with previous reports of piperlongumine-induced apoptosis in TNBC cells (15,17). Moreover, we show here for the first time that treatment of highly aggressive MDA-MB-231 TNBC cells with a sub-cytotoxic concentration of piperlongumine

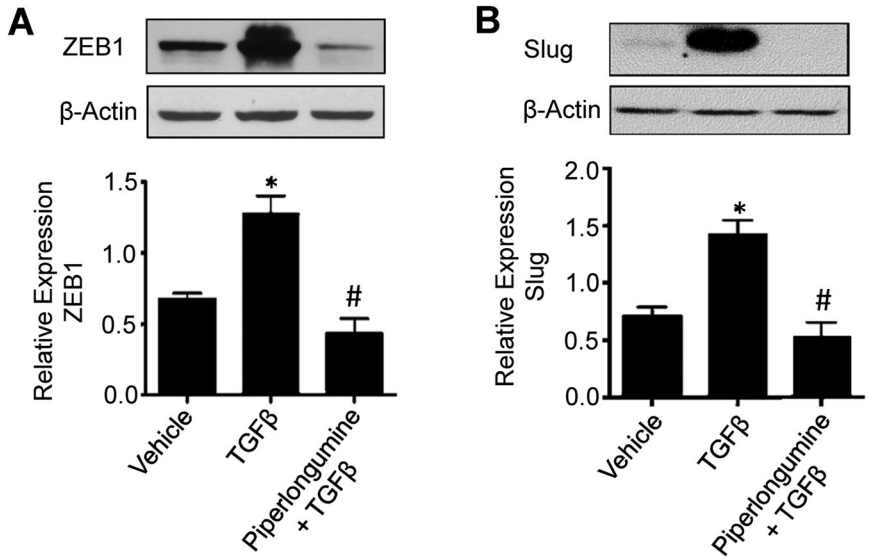

Figure 5. Piperlongumine inhibits TGFβ-induced ZEB1 and Slug expression by TNBC cells. MDA-MB-231 cells were cultured for 48 h in the presence of 1 ng/ml of TGFβ treated with or without 2.5 μM piperlongumine. Cell lysates were collected and the expression of (A) ZEB1 and (B) Slug were determined by western blotting and densitometry. β-actin expression was determined to confirm equal loading of proteins. Representative blots are shown. (A, B) Data shown are the average of 3 independent experiments ± SEM. Statistical significance was determined by ANOVA with Tukey's post-hoc test; * denotes $p < 0.05$ relative to the vehicle control; # denotes $p < 0.05$ relative to TGFβ-treated cells.

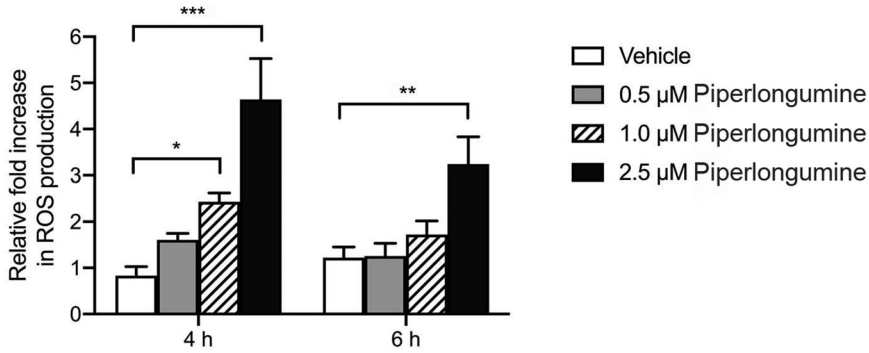

Figure 6. Piperlongumine induces ROS accumulation in TNBC cells. MDA-MB-231 cells were stained with DCFDA and treated with vehicle (DMSO) or the indicated concentrations of piperlongumine for 4 or 6 h. Cells were then harvested and DCFDA fluorescence intensity was measured. Data shown are the mean relative fold increase in ROS production ± SEM of 3 independent experiments. Statistical significance was determined by ANOVA with Tukey's post-hoc test; * $p < 0.05$, ** $p < 0.001$, and *** $p < 0.0001$ relative to the vehicle control.

suppressed the in vitro and in vivo metastatic activity of these TNBC cells and altered their expression of EMT- and metastasis-associated proteins in a ROS-dependent fashion.

Sub-cytotoxic piperlongumine inhibited the migration of MDA-MB-231 cells in a gap closure assay and interfered with invasion of MDA-MB-231 cells through a fibronectin-coated membrane. Low dose piperlongumine also suppressed the expression of MMP2 and MMP9, both of which facilitate cancer cell invasion into surrounding tissues and are associated with a poor prognosis (20,21). MMP2 and MMP9 expression by breast cancer cells is upregulated by the TGFβ pathway, thereby promoting TGFβ-induced metastasis of malignant breast epithelial cells (22). These findings suggest that piperlongumine has the potential to interfere with breast cancer spread to secondary sites since tumor cell motility/invasion and the degradation of extracellular matrix components play essential roles in metastasis.

Although a critical role for EMT in metastasis formation has been questioned (23), numerous studies using human cancer cell lines, mouse models of cancer, and clinical isolates of human cancer tissue support the importance of transient EMT for effective metastasis (24). The MDA-MB-231 TNBC cell line is characterized by a mesenchymal-like phenotype (25); however, MDA-MB-231 cells became more epithelial-

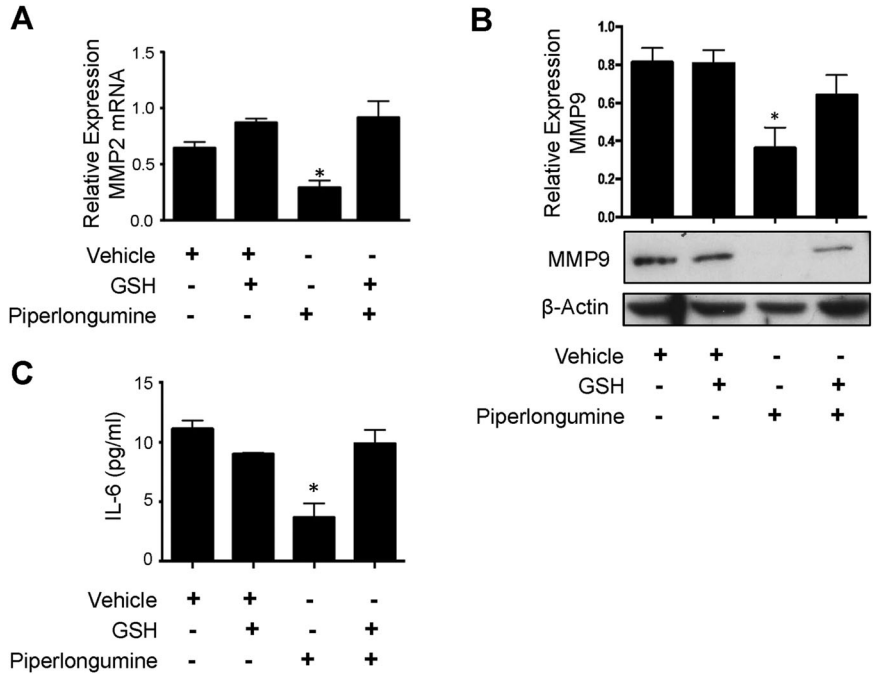

Figure 7. GSH prevents piperlongumine-induced inhibition of MMP-2, MMP-9 and IL-6 expression. MDA-MB-231 cells were treated with 10 mM GSH or medium alone for 1 h prior to the addition of medium, vehicle (DMSO), or 1 μM (A) or 2.5 μM (B, C) piperlongumine. Cells were then cultured for 48 h. (A) MMP2 mRNA was measured using RT-qPCR. (B) Cell lysates were prepared, and western blotting was used to measure MMP9 protein. (C) Cell culture supernatants were collected and secreted IL-6 was measured by ELISA. (A, B, C) Data shown are the means of 3 independent experiments ± SEM. Statistical significance relative to the vehicle control was determined by ANOVA with Tukey's post-hoc test; * denotes $p < 0.05$.

like following treatment with low dose piperlongumine. This was in line with the finding that expression of the EMT-promoting transcription factors ZEB1 and Slug was decreased in piperlongumine-treated MDA-MB-231 cells. In addition, TGFβ-induced expression of ZEB1 and Slug by MDA-MB-231 cells was abrogated in the presence of piperlongumine. This suggests that piperlongumine inhibits the TGFβ signaling pathway, which plays a key role in stimulating EMT, upregulating MMP2 and MMP9 expression, and promoting cancer progression (5,6,22). In contrast, piperlongumine-treated MDA-MB-231 cells showed increased expression of mRNA coding for E-cadherin, which is an adhesion molecule and epithelial marker (26). Loss or disruption of E-cadherin is critical for tumor initiation and progression (27), and dysregulated E-cadherin expression is associated with poor outcomes in breast cancer patients (28). Decreased ZEB1 and Slug expression by piperlongumine-treated MDA-MB-231 cells likely accounts for increased expression of E-cadherin since both ZEB1 and Slug are transcriptional repressors of E-cadherin (29,30).

We also observed that exposure to piperlongumine caused MDA-MB-231 cells to upregulate their expression of miR-200c, which is consistent with the reported upregulation of miR-200c transcription following ZEB1 knockdown in MDA-MB-231 cells (31). Transcription of miR-200 family members strongly correlates with E-cadherin expression and an epithelial phenotype in cancer cells, which is thought to result from their direct targeting and suppression of ZEB1 and ZEB2 (32). Interestingly, ZEB1 represses miR-200c transcription in a reciprocal fashion, which is hypothesized to result in a "feedforward loop" that stabilizes EMT and an invasive phenotype (31). Since reverting MDA-MB-231 TNBC cells from mesenchymal to epithelial morphology reduces their ability to migrate and invade (33), the ability of low dose piperlongumine to suppress EMT-associated ZEB1 and Slug expression while promoting an epithelial phenotype via increased miR-200c transcription and E-cadherin expression suggests that piperlongumine may be able to reverse EMT in TNBC cells and thereby prevent or reduce metastasis.

Exposure of MDA-MB-231 TNBC cells to sub-cytotoxic piperlongumine caused a dramatic reduction in the synthesis of inflammation-promoting IL-6, which is a key cytokine in the progression of TNBC (34). In this regard, IL-6 is important for the aggressive nature of MDA-MB-231 cells and induces EMT and stemness in less aggressive MCF-7 breast cancer cells (35). IL-6

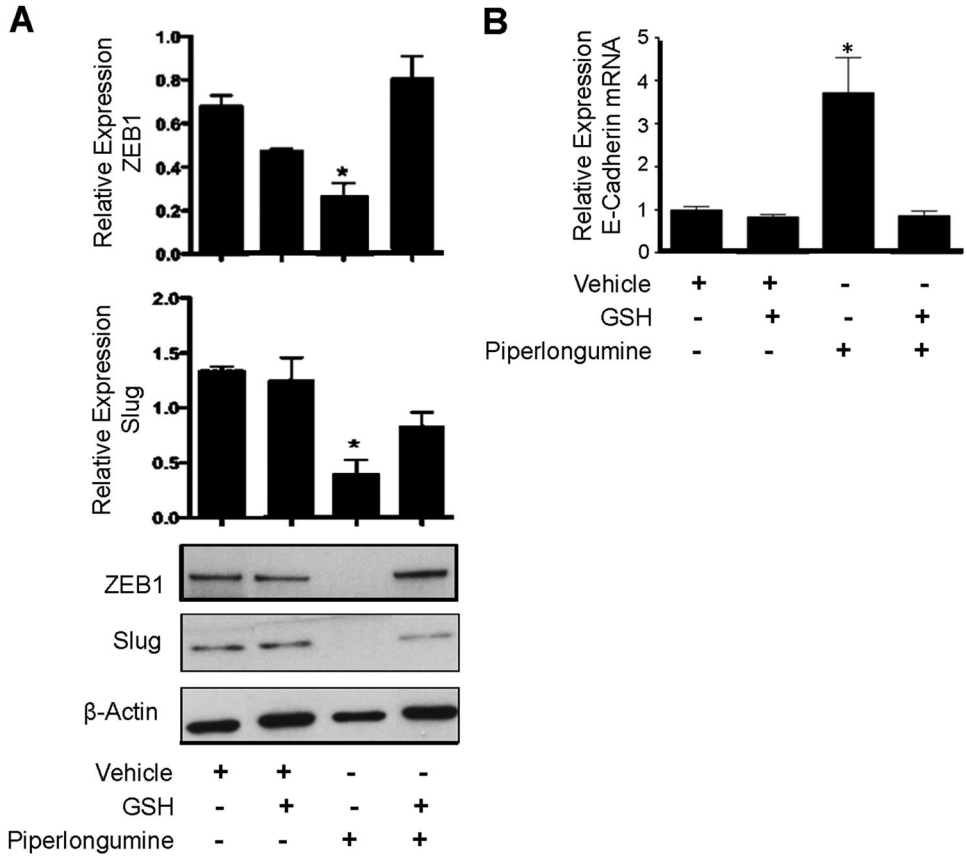

Figure 8. GSH prevents piperlongumine-induced modulation of ZEB1, Slug, and E-cadherin expression. MDA-MB-231 cells were treated with 10 mM GSH or medium alone for 1 h prior to the addition of medium, vehicle (DMSO), or 2.5 μM piperlongumine,. Cells were then cultured for (A) 48 h or (B) 72 h. (A) Cell lysates were prepared, and western blotting was used to measure ZEB1 and Slug protein; β-actin expression was determined to confirm equal loading of proteins. (B) E-cadherin mRNA was measured using RT-qPCR. Data shown are the means of 3 independent experiments ± SEM. Statistical significance relative to the vehicle control was determined by ANOVA with Tukey's post-hoc test; * denotes $p < 0.05$.

is also among the TNBC cell-elaborated soluble factors that stimulate metastasis-promoting angiogenesis and recruit immunosuppressive myeloid cells to the tumor microenvironment (36). It is no surprise that high levels of circulating IL-6 are associated with poor prognosis in TNBC (37). Reduced expression of ZEB1 may account for decreased IL-6 synthesis by piperlongumine-treated MDA-MB-231 cells since ZEB1 is a key transcriptional regulator of pro-inflammatory IL-6 (38).

Consistent with our in vitro finding of reduced metastatic potential following piperlongumine treatment of MDA-MB-231 TNBC cells, we found that piperlongumine-treated 4T1 mammary carcinoma-bearing BALB/c mice had significantly fewer lung metastases than control animals. The orthotopic 4T1 mouse mammary carcinoma model may be a more accurate representation of human breast cancer metastasis, as more tumors metastasize successfully from the mammary fat pad in the presence of a functional immune system (19). Expression of the Ki67 proliferation marker within primary tumors was not affected by piperlongumine treatment nor was tumor size significantly reduced in comparison to control tumors. These findings are consistent with mice receiving a sub-cytotoxic dose of piperlongumine. However, MMP2 expression was significantly reduced in primary tumors from the piperlongumine-treated group, which was in line with decreased MMP2 expression by MDA-MB-231 cells following treatment with low dose piperlongumine.

Estrogen receptor-bearing MCF-7 breast cancer cultured in the presence of piperlongumine experience GSH depletion and ROS accumulation (39). We observed that MDA-MB-231 TNBC cells treated with low dose piperlongumine also exhibited ROS accumulation. Moreover, the addition of exogenous GSH to piperine-treated MDA-MB-231 cells restored MMP2, MM9, IL-6, ZEB1 and Slug expression to control levels, as well as preventing any increased expression of E-cadherin. These findings indicated that piperlongumine-induced ROS accumulation was responsible for

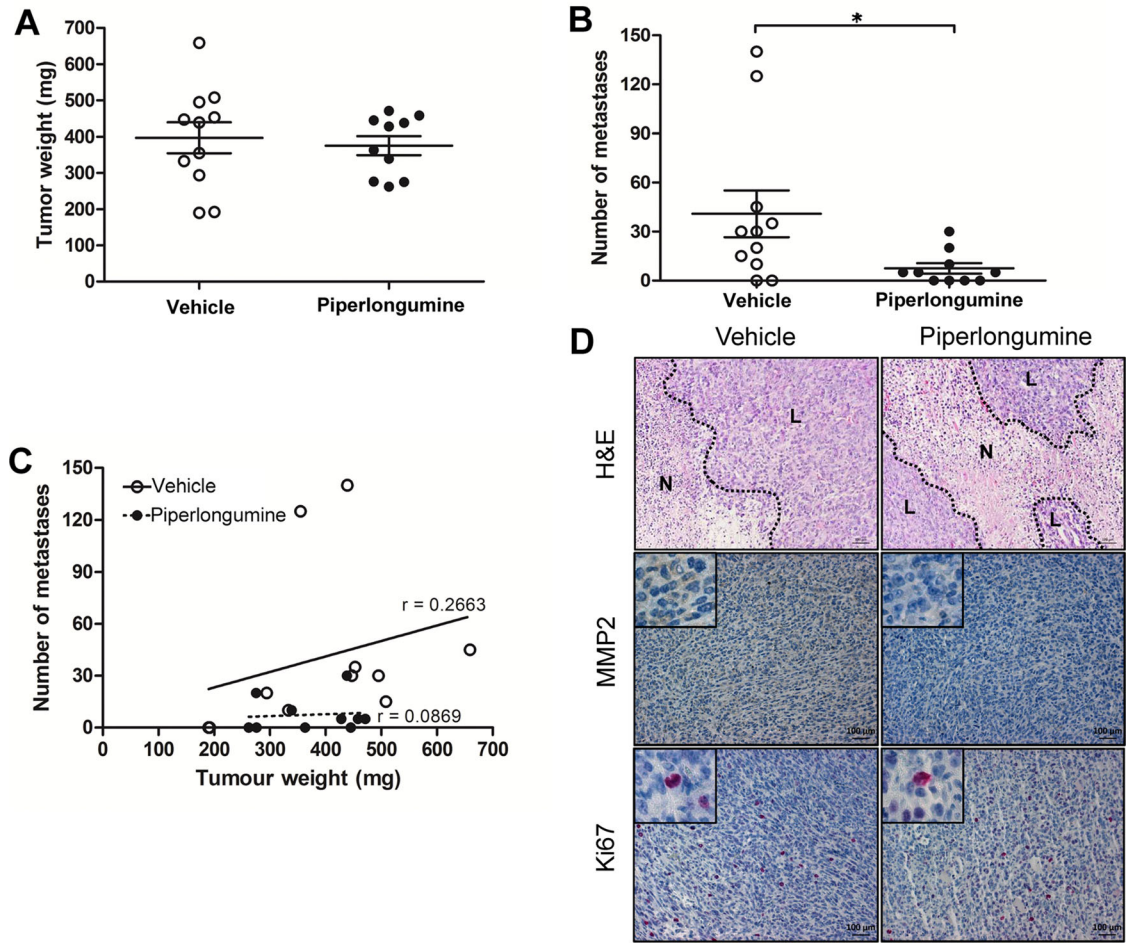

Figure 9. Piperlongumine reduces triple-negative murine mammary carcinoma cell metastasis to the lungs. BALB/c mice received a subcutaneous injection of 4T1 mammary carcinoma cells in the right flank. Once tumors reached 100 mm^3, mice received a daily intraperitoneal injection of vehicle (DMSO) or piperlongumine (2.5 mg/kg) for 9 days. (A) Primary tumors were excised from euthanized mice and tumor weights were recorded. (B) Lung tissue was homogenized and digested, then cultured for 14 days in 6-thioguanine-containing medium to select for 4T1 cells. At the end of culture, 4T1 colonies were stained with crystal violet and counted. (C) The correlation coefficient (r) for primary tumor weight and number of lung metastases was calculated. (D) Primary tumors were fixed in formalin and sectioned. Regions of tumors containing live (L) and necrotic (N) cells were identified by hematoxylin and eosin (H&E) staining. MMP2 and Ki67 expression was determined by immunohistochemistry. The control group consisted of 11 mice and the treatment group consisted of 10 mice. Points on the graph represent measurements from each mouse; error bars represent SEM. Statistical significance was determined using Student's t-test; * denotes $p < 0.05$.

the inhibitory effect of sub-cytotoxic piperlongumine on EMT-associated metastatic activity of MDA-MB-231 cells. Although the mechanism by which piperlongumine caused intracellular ROS accumulation is not clear at this time, it is known that piperlongumine inhibits the enzymatic activity of detoxifying glutathione S-transferase pi 1 in cancer cells via formation of a hydrolyzed piperlongumine-GSH conjugate that blocks the active site of the enzyme (40). The resulting depletion of ROS-scavenging GSH would be expected to cause oxidative stress due to the accumulation of intracellular ROS, which is already present at higher than normal levels in cancer cells (9).

In conclusion, this study reveals previously undescribed effects of sub-cytotoxic piperlongumine on EMT-associated molecules and metastatic activities of TNBC cells. The expression of metastasis-promoting molecules (IL-6, MMP2, MMP9, ZEB1, Slug) was downregulated whereas metastasis-suppressing molecules (miR-200c, E-cadherin) showed increased expression in the presence of piperlongumine. These effects were dependent on piperlongumine-induced accumulation of intracellular ROS since they were largely reversed in the presence of exogenous GSH. The in vitro and in vivo antimetastatic effects of piperlongumine on TNBC cells, in combination with its capacity to increase TNBC sensitivity to chemotherapeutic agents and ionizing radiation (41,42), suggest that piperlongumine may be useful in the treatment of TNBC.

Acknowledgments

The authors acknowledge Pat Colp for assistance with histology and immunohistochemistry.

Contributions

Overall design of study: David W. Hoskin

Experiment design and conduct: Leanne M Delaney, Nathan Farias, Javad Ghassemi Rad, Wasundara Fernando, Henry Annan

Data analysis: Leanne M Delaney, Nathan Farias, Javad Ghassemi Rad, Wasundara Fernando, Henry Annan

Manuscript preparation: Leanne M Delaney, Javad Ghassemi Rad, Wasundara Fernando

Manuscript editing: David W. Hoskin

Disclosure Statement

The authors report no conflict of interest.

Funding

This work was funded by the Canadian Cancer Society, grant 314347.

References

1. Foulkes WD, Smith IE, Reis-Filho JS. Triple-negative breast cancer. N Engl J Med. 2010;363(20):1938–48. doi:10.1056/NEJMra1001389
2. Kotiyal S, Bhattacharya S. Breast cancer stem cells, EMT and therapeutic targets. Biochem Biophys Res Commun. 2014;453(1):112–6. doi:10.1016/j.bbrc.2014.09.069
3. Dongre A, Weinberg RA. New insights into the mechanisms of epithelial-mesenchymal transition and implications for cancer. Nat Rev Mol Cell Biol. 2019;20(2):69–84. doi:10.1038/s41580-018-0080-4
4. Almendro V, Kim HJ, Cheng Y-K, Gönen M, Itzkovitz S, Argani P, van Oudenaarden A, Sukumar S, Michor F, Polyak K, et al. Genetic and phenotypic diversity in breast tumor metastases. Cancer Res. 2014;74(5):1338–48. doi:10.1158/0008-5472.CAN-13-2357-T
5. Hao Y, Baker D, Dijke PT. TGF-β-mediated epithelial-mesenchymal transition and cancer metastasis. IJMS. 2019;20(11):2767. doi:10.3390/ijms20112767
6. Katsuno Y, Lamouille S, Derynck R. TGF-β signaling and epithelial-mesenchymal transition in cancer progression. Curr Opin Oncol. 2013;25(1):76–84. doi:10.1097/CCO.0b013e32835b6371
7. Radisky ES, Radisky DC. Matrix metalloproteinase-induced epithelial-mesenchymal transition in breast cancer. J Mammary Gland Biol Neoplasia. 2010;15(2):201–12. doi:10.1007/s10911-010-9177-x
8. Prasad S, Tyagi A. Historical spice as a future drug: therapeutic potential of piperlongumine. Curr Pharm Des. 2016;22(27):4151–9. doi:10.2174/1381612822666160601103027
9. Jin H-O, Lee Y-H, Park J-A, Lee H-N, Kim J-H, Kim J-Y, Kim BRa, Hong S-E, Kim H-A, Kim E-K, et al. Piperlongumine induces cell death through ROS-mediated CHOP activation and potentiates TRAIL-induced cell death in breast cancer cells. J Cancer Res Clin Oncol. 2014;140(12):2039–46. doi:10.1007/s00432-014-1777-1
10. Park J-A, Na H-H, Jin H-O, Kim K-C. Increased expression of FosB through reactive oxygen species accumulation functions as pro-apoptotic protein in piperlongumine Treated MCF7 Breast Cancer Cells. Mol Cells. 2019;42(12):884–92. doi:10.14348/molcells.2019.0088
11. Liu JM, Pan F, Li L, Liu QR, Chen Y, Xiong XX, Cheng K, Yu SB, Shi Z, Yu AC-H, et al. Piperlongumine selectively kills glioblastoma multiforme cells via reactive oxygen species accumulation dependent JNK and p38 activation. Biochem Biophys Res Commun. 2013;437(1):87–93. doi:10.1016/j.bbrc.2013.06.042
12. Roh J-L, Kim EH, Park JY, Kim JW, Kwon M, Lee B-H. Piperlongumine selectively kills cancer cells and increases cisplatin antitumor activity in head and neck cancer. Oncotarget. 2014;5(19):9227–38. doi:10.18632/oncotarget.2402
13. Huang BK, Langford TF, Sikes HD. Using sensors and generators of H_2O_2 to elucidate the toxicity mechanism of piperlongumine and phenethyl isothiocyanate. Antioxid Redox Signal. 2016;24(16):924–38. doi:10.1089/ars.2015.6482
14. Wang J, Yi J. Cancer cell killing via ROS: to increase or decrease, that is the question. Cancer Biol Ther. 2008;7(12):1875–84. doi:10.4161/cbt.7.12.7067
15. Chen D, Ma Y, Li P, Liu M, Fang Y, Zhang J, Zhang B, Hui Y, Yin Y. Piperlongumine induces apoptosis and synergizes with doxorubicin by inhibiting the JAK2-STAT3 pathway in triple-negative breast cancer. Molecules. 2019;24(12):2338. doi:10.3390/molecules24122338
16. Niu M, Shen Y, Xu X, Yao Y, Fu C, Yan Z, Wu Q, Cao J, Sang W, Zeng L, et al. Piperlongumine selectively suppresses ABC-DLBCL through inhibition of NF-κB p65 subunit nuclear import. Biochem Biophys Res Commun. 2015;462(4):326–31. doi:10.1016/j.bbrc.2015.04.136
17. Shrivastava S, Kulkarni P, Thummuri D, Jeengar MK, Naidu VGM, Alvala M, Redddy GB, Ramakrishna S. Piperlongumine, an alkaloid causes inhibition of PI3 K/Akt/mTOR signaling axis to induce caspase-dependent apoptosis in human triple-negative breast cancer cells . Apoptosis. 2014;19(7):1148–64. doi:10.1007/s10495-014-0991-2
18. Niu M, Xu X, Shen Y, Yao Y, Qiao J, Zhu F, Zeng L, Liu X, Xu K. Piperlongumine is a novel nuclear export inhibitor with potent anticancer activity. Chem Biol Interact. 2015;237:66–72. doi:10.1016/j.cbi.2015.05.016
19. Pulaski BA, Ostrand-Rosenberg S. Mouse 4T1 breast tumor model. Curr Protoc Immunol. 2001; Unit 20.2. doi:10.1002/0471142735.im2002s39

20. Zhang F, Wang Z, Fan Y, Xu Q, Ji W, Tian R, Niu R. Elevated STAT3 signaling-mediated upregulation of MMP-2/9 confers enhanced invasion ability in multidrug-resistant breast cancer cells. Int J Mol Sci. 2015; 16(10):24772–90. doi:10.3390/ijms161024772
21. Ren F, Tang R, Zhang X, Madushi WM, Luo D, Dang Y, Li Z, Wei K, Chen G. Overexpression of MMP family members functions as prognostic biomarker for breast cancer patients: a systemic review and meta-analysis. PLoS One. 2015;10(8):e0135544. doi:10.1371/journal.pone.0135544
22. Wiercinska E, Naber HP, Pardali E, van der Pluijm G, van Dam H, ten Dijke P. The TGF-β/Smad pathway induces breast cancer cell invasion through the up-regulation of matrix metalloproteinase 2 and 9 in a spheroid invasion model system. Breast Cancer Res Treat. 2011;128(3):657–66. doi:10.1007/s10549-010-1147-x
23. Diepenbruck M, Christofori G. Epithelial-mesenchymal transition (EMT) and metastasis: yes, no, maybe?. Curr Opin Cell Biol. 2016;43:7–13. doi:10.1016/j.ceb.2016.06.002
24. Yeung KT, Yang J. Epithelial-mesenchymal transition in tumor metastasis. Mol Oncol. 2017;11(1):28–39. doi:10.1002/1878-0261.12017
25. Law ME, Corsino PE, Jahn SC, Davis BJ, Chen S, Patel B, Pham K, Lu J, Sheppard B, Nørgaard P, et al. Glucocorticoids and histone deacetylase inhibitors cooperate to block the invasiveness of basal-like breast cancer cells through novel mechanisms. Oncogene. 2013;32(10):1316–29. doi:10.1038/onc.2012.138
26. Gheldof A, Berx G. Cadherins and epithelial-to-mesenchymal transition. Prog Mol Biol Transl Sci. 2013; 116:317–36. doi:10.1016/B978-0-12-394311-8.00014-5
27. Kourtidis A, Lu R, Pence LJ, Anastasiadis PZ. Anastasiadis PZ: A central role for cadherin signaling in cancer. Exp Cell Res. 2017;358(1):78–85. doi:10.1016/j.yexcr.2017.04.006
28. Liu T, Zhang X, Shang M, Zhang Y, Xia B, Niu M, Liu Y, Pang D. Dysregulated expression of Slug, vimentin, and E-cadherin correlates with poor clinical outcome in patients with basal-like breast cancer. J Surg Oncol. 2013;107(2):188–94. doi:10.1002/jso.23240
29. Hajra KM, Chen DY, Fearon ER. The SLUG zinc-finger protein represses E-cadherin in breast cancer. Cancer Res. 2002;62(6):1613–8.
30. Mazda M, Nishi K, Naito Y, Ui-Tei K. E-cadherin is transcriptionally activated via suppression of ZEB1 transcriptional repressor by small RNA-mediated gene silencing. PLoS One. 2011;6(12):e28688doi:10.1371/journal.pone.0028688
31. Burk U, Schubert J, Wellner U, Schmalhofer O, Vincan E, Spaderna S, Brabletz T. A reciprocal repression between ZEB1 and members of the miR-200 family promotes EMT and invasion in cancer cells. EMBO Rep. 2008;9(6):582–9. doi:10.1038/embor.2008.74
32. Park S-M, Gaur AB, Lengyel E, Peter ME. The miR-200 family determines the epithelial phenotype of cancer cells by targeting the E-cadherin repressors ZEB1 and ZEB2. Genes Dev. 2008;22(7):894–907. doi:10.1101/gad.1640608
33. Chao YL, Shepard CR, Wells A. Breast carcinoma cells re-express E-cadherin during mesenchymal to epithelial reverting transition. Mol Cancer. 2010;9:179. doi:10.1186/1476-4598-9-179
34. Hartman ZC, Poage GM, den Hollander P, Tsimelzon A, Hill J, Panupinthu N, Zhang Y, Mazumdar A, Hilsenbeck SG, Mills GB, et al. Growth of triple-negative breast cancer cells relies upon coordinate autocrine expression of the proinflammatory cytokines IL-6 and IL-8. Cancer Res. 2013;73(11): 3470–80.,. doi:10.1158/0008-5472.CAN-12-4524-T
35. Ortiz-Montero P, Londono-Vallejo A, Vernot JP. Senescence-associated IL-6 and IL-8 cytokines induce a self- and cross-reinforced senescence/inflammatory milieu strengthening tumorigenic capabilities in the MCF-7 breast cancer cell line. Cell Commun Signal. 2017;15(1):17doi:10.1186/s12964-017-0172-3
36. Suarez-Carmona M, Bourcy M, Lesage J, Leroi N, Syne L, Blacher S, Hubert P, Erpicum C, Foidart J-M, Delvenne P, et al. Soluble factors regulated by epithelial-mesenchymal transition mediate tumour angiogenesis and myeloid cell recruitment. J Pathol. 2015; 236(4):491–504.,. doi:10.1002/path.4546
37. Salgado R, Junius S, Benoy I, Van Dam P, Vermeulen P, Van Marck E, Huget P, Dirix LY. Circulating interleukin-6 predicts survival in patients with metastatic breast cancer. Int J Cancer. 2003;103(5):642–6. doi:10.1002/ijc.10833
38. Katsura A, Tamura Y, Hokari S, Harada M, Morikawa M, Sakurai T, Takahashi K, Mizutani A, Nishida J, Yokoyama Y, et al. ZEB1-regulated inflammatory phenotype in breast cancer cells. Mol Oncol. 2017;11(9):1241–62.,. doi:10.1002/1878-0261.12098
39. Jeong CH, Ryu H, Kim DH, Cheng WN, Yoon JE, Kang S, Han SG. Piperlongumine induces cell cycle arrest via reactive oxygen species accumulation and IKKβ suppression in human breast cancer cells. Antioxidants. 2019;8(11):553. doi:10.3390/antiox8110553
40. Harshbarger W, Gondi S, Ficarro SB, Hunter J, Udayakumar D, Gurbani D, Singer WD, Liu Y, Li L, Marto JA, et al. Structural and biochemical analyses reveal the mechanism of glutathione S-transferase pi 1 inhibition by the anti-cancer compound piperlongumine. J Biol Chem. 2017;292(1):112–20. doi:10.1074/jbc.M116.750299
41. Patel K, Chowdhury N, Doddapaneni R, Boakye CHA, Godugu C, Singh M. Piperlongumine for enhancing oral bioavailability and cytotoxicity of docetaxel in triple-negative breast cancer. J Pharm Sci. 2015;104(12):4417–26. doi:10.1002/jps.24637
42. Yao JX, Yao ZF, Li ZF, Liu YB. Radio-sensitization by Piper longumine of human breast adenoma MDA-MB-231 cells in vitro. Asian Pac J Cancer Prev. 2014; 15(7):3211–7. doi:10.7314/apjcp.2014.15.7.3211